Influence of AlN interlayer on the anisotropic electron mobility and the device characteristics of N-polar AlGaN/GaN metal-insulator-semiconductor-high electron mobility transistors grown on vicinal substrates

Seshadri Kolluri,[1,a)] Stacia Keller,[1] David Brown,[1] Geetak Gupta,[1] Umesh K. Mishra,[1] Steven P. Denbaars,[2] and Siddharth Rajan[3]
[1]*Department of Electrical and Computer Engineering, University of California, Santa Barbara, California 93106, USA*
[2]*Department of Materials, University of California, Santa Barbara, California 93106, USA*
[3]*Department of Electrical and Computer Engineering, Ohio State University, Columbus, Ohio 43210, USA*

(Received 4 May 2010; accepted 10 August 2010; published online 5 October 2010)

This paper presents an experimental investigation of the influence of an AlN interlayer on the electron mobility and the device characteristics of N-polar AlGaN/GaN metal-insulator-semiconductor-high electron mobility transistors grown by metal-organic chemical vapor deposition on miscut sapphire substrates. Use of miscut substrates leads to the formation of multiatomic steps at the AlGaN/GaN interface and anisotropy in electron transport properties. A combination of van der Pauw Hall, gated transfer length measurements, and capacitance-voltage measurements has been used to study the desired properties in directions parallel and perpendicular to the multiatomic steps and qualitative explanations were provided for the observed trends. Similar to the Ga-polar devices, the introduction of AlN interlayer improved the device performance by increasing both the electron mobility and the two-dimensional electron gas charge density in the devices. Orienting the devices such that the conduction occurred parallel to the multiatomic steps was beneficial for better electron transport and device performance. © *2010 American Institute of Physics*. [doi:10.1063/1.3488641]

I. INTRODUCTION

AlGaN/GaN high electron mobility transistors (HEMTs) have great potential for high-power microwave applications due to the large band gap of GaN, high electron mobility, and high sheet carrier density of AlGaN/GaN heterostructures.[1] The high breakdown voltage of the nitride material system, together with the development of field-plate and passivation technologies, has enabled devices with continuous wave output power densities in excess of 40 W/mm at 4 GHz and 20 W/mm at 10 GHz.[2,3] Aggressive reduction in the gate length down to sub-100 nm and the corresponding scaling of device aspect ratio have led to high intrinsic current- and power-gain cutoff frequencies (f_T and f_{max}) of 190 GHz and 251 GHz, respectively.[4]

Compared to Ga-polar GaN devices, N-polar (N-face) devices potentially offer several advantages such as lower contact resistance[5] and better electron confinement.[6] However, most of the earlier device research was focused on Ga-polar devices, while N-polar devices received little attention due to several growth related issues.[7,8] Over the last few years, significant progress has been achieved in the growth of N-polar devices by both molecular beam epitaxy (MBE) (Ref. 9) and metal-organic chemical vapor deposition (MOCVD).[10,11] Particularly, for the growth of N-polar HEMTs by MOCVD, use of misoriented (vicinal) sapphire substrates was required to minimize the formation of hexagonal hillocks on the surface.[10] Growth on vicinal substrate results in formation of multiatomic steps at the AlGaN/GaN interface. Increased interface roughness scattering for conduction perpendicular to these multiatomic steps leads to degradation of electron mobility in that direction and causes a strong anisotropy in electron transport properties, which will be discussed in the later sections.

With recent developments in device design and processing of N-polar HEMTs, rf power performance with a power added efficiency comparable to Ga-polar devices has been achieved by both MBE (Ref. 12) and MOCVD.[13] Future progress in the N-polar GaN technology depends on additional developments in improving the current carrying capacity of the devices. One of the primary factors influencing the current carrying capacity of the devices is the two-dimensional electron gas (2DEG) conductivity, which is proportional to the product of electron mobility (μ_e) and carrier sheet charge density (n_s). Though using a higher Al mole fraction in the AlGaN back barrier is desirable for increasing the carrier sheet charge density, it adversely affects the electron mobility, due to increased alloy disorder scattering. Previous investigations on Ga-polar heterostructures showed that the introduction of an AlN interlayer helps mitigate this alloy disorder scattering by moving ternary AlGaN layer away from the 2DEG.[14]

In this article, we present an experimental investigation of influence of channel orientation on the electron mobility and device characteristics of N-polar AlGaN/GaN metal-insulator-semiconductor-HEMTs, as well as the improve-

[a)]Electronic mail: seshadri@ece.ucsb.edu.

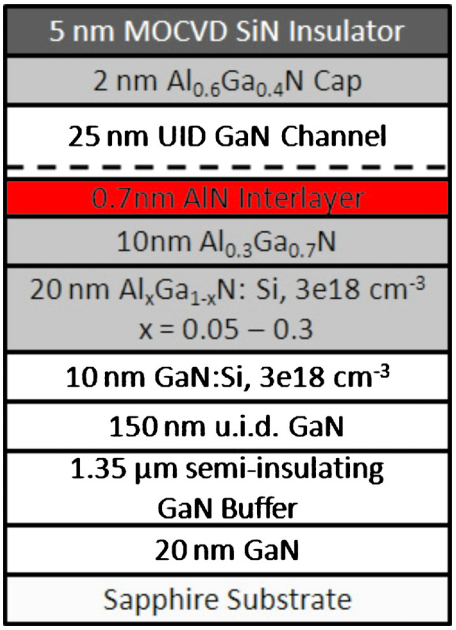

FIG. 1. (Color online) Epitaxial structure of the device.

ments obtained by the introduction of an AlN interlayer in both the directions parallel and perpendicular to the multiatomic steps. A combination of van der Pauw Hall, gated transfer length measurements (gated TLMs), and capacitance-voltage (C-V) measurements was used to study the desired properties. The details of the device structure, processing, measurements, and analysis of the results will be presented in the following sections.

II. EXPERIMENT

In this study, samples of epitaxial structure shown in Fig. 1, with and without the 0.7 nm AlN interlayer were investigated. The N-polar HEMT structures were grown by MOCVD using trimethylgallium, trimethylaluminum, and ammonia as precursors on (0001) sapphire with a misorientation angle of 4° toward the a-sapphire-plane.[10,11] The GaN deposition was initiated with the growth of a 20 nm thick unintentionally doped (u.i.d.) GaN layer. Next, a 1.35 μm thick semi-insulating GaN layer was grown, using bis-cyclopentadienyl-iron $[(Cp)_2Fe]$ to render the layer semi-insulating.[15] On top of the Fe-doped layer, a 0.15 μm thick u.i.d. GaN spacer layer was deposited, followed by a 10 nm thick silicon doped layer with a free carrier concentration of 3×10^{18} cm^{-3} using disilane as precursor. Next, a 20 nm thick $Al_xGa_{1-x}N$:Si layer was grown, where x_{Al} was graded from 0.05 to 0.3. The disilane flow was adjusted to render a constant Si doping level of 3×10^{18} cm^{-3}. On top of the graded AlGaN layer, a 10 nm thick u.i.d. $Al_{0.3}Ga_{0.7}N$ was deposited, followed by a 0.7 nm AlN interlayer for one sample and no inter layer another sample. Next, a 25 nm thick u.i.d. GaN channel layer was grown. The layer structure was finished with a 2 nm thick $Al_{0.6}Ga_{0.4}N$ cap layer to reduce gate leakage. To further reduce the gate leakage, a 5 nm thick *in situ* silicon nitride layer was deposited over the $Al_{0.6}Ga_{0.4}N$ cap. Additional details on the growth procedure can be found in Keller *et al.*[11]

The HEMTs were fabricated by standard photolithography. A Ti/Al/Ni/Au (20/100/10/50 nm) multilayered stack, annealed at 870 °C for 30 s in a N_2 atmosphere, was used for Ohmic metallization. Mesas were formed with BCl_3/Cl_2 reactive ion etch. Next, gates were formed using e-beam evaporation with a stack of Ni/Au/Ni (30/250/50 nm). The surface was subsequently passivated with 160 nm Si_xN_y by plasma-enhanced CVD. The devices under investigation had a width of 2×75 μm and a gate length of 0.7 μm. The gate-to-source spacing is 0.5 μm and gate-to-drain spacing was 2 μm.

III. RESULTS AND DISCUSSION

Figure 2 shows the simulated band diagrams for the devices with and without the interlayer, obtained using a one-dimensional Schrödinger–Poisson solver.[16] It can be observed that the AlN interlayer separates the channel from the ternary AlGaN layer and also provides higher back barrier confinement for the electrons in the channel. van der Pauw Hall and TLM patterns in both directions were used to calculate the 2DEG concentration, sheet resistance, and electron mobility values for conduction parallel and perpendicular to multiatomic steps. As seen in Fig. 3, insertion of an AlN interlayer resulted in higher mobility values for in both directions. The 2DEG concentration increased slightly as well,

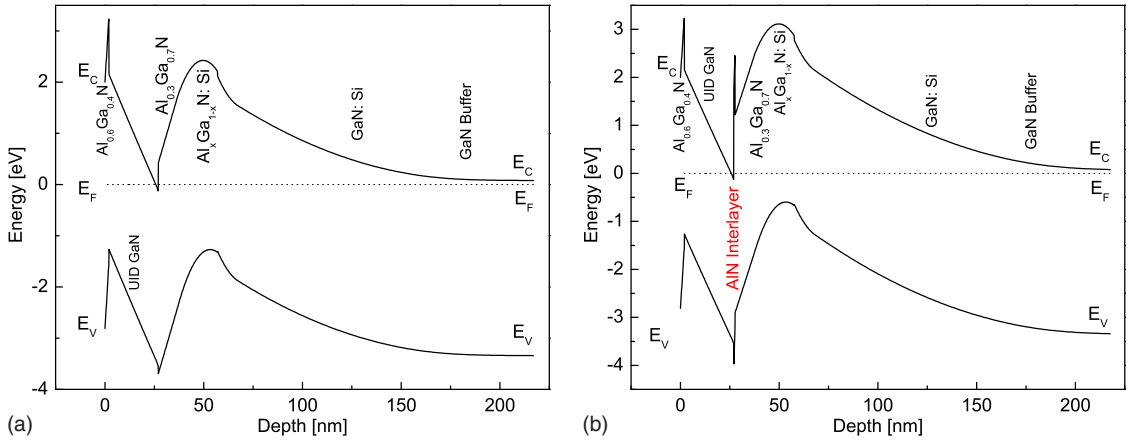

FIG. 2. (Color online) Simulated band diagrams of the devices: (a) without the interlayer and (b) with the interlayer.

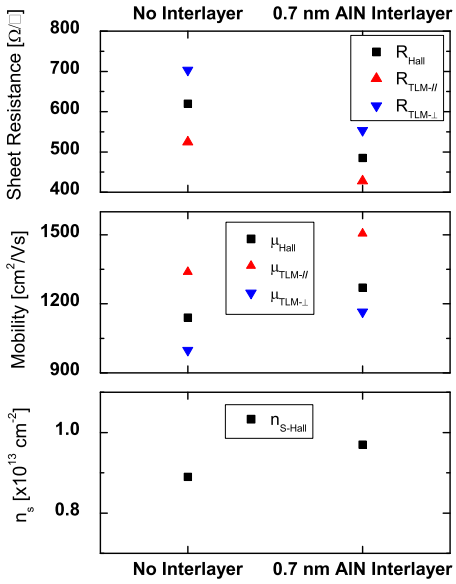

FIG. 3. (Color online) Electron concentration, directional dependent mobility, and sheet resistance values calculated from van der Pauw Hall and TLM measurements.

because of additional polarization due to the AlN interlayer. Figure 3 also shows that the mobility values for conduction parallel to the multiatomic steps are significantly higher than those for the conduction perpendicular to the steps. This results in a lower sheet resistance for conduction parallel to the steps.

The differences observed in the mobility and sheet resistance were also reflected in corresponding trends in on-resistance (R_{ON}) and on-current (I_{ON}) of the devices, as depicted in Fig. 4. Introduction of an AlN interlayer improved the R_{ON} and I_{ON} values by more than 10%, for devices oriented both parallel and perpendicular to the steps. Best results were obtained for the devices which had an AlN interlayer and were oriented such that the device conduction is parallel to the multiatomic steps.

As shown in Fig. 5, the interlayer did not have a significant effect on the pinch-off voltage of the devices. However, it was observed that there was a difference of about 1 V in the pinch-off voltages of devices oriented parallel and perpendicular to the multiatomic steps, on the same sample. This anisotropy in pinch-off voltage with respect to device orientation was observed earlier[17,18] and difference was attributed to a potential modulation by the multiatomic steps, which would cause an additional confinement for electronic conduction across the multiatomic steps. This anisotropy in pinch-off voltage is also consistent with similar observations in AlGaAs/GaAs heterostructures grown on vicinal substrates.[19]

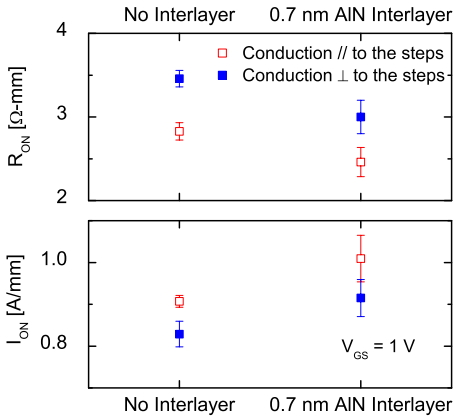

FIG. 4. (Color online) Influence of AlN interlayer on on-current (I_{ON}, at V_{GS}=1 V) and on-resistance (R_{ON}) of the devices. Error bars denote the die-to-die variations in within the samples.

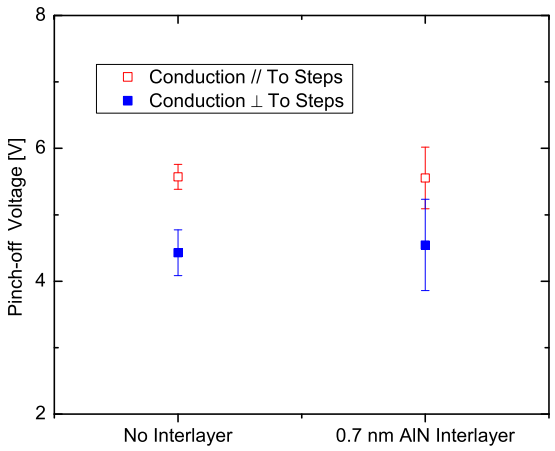

FIG. 5. (Color online) Variation in the pinch-off voltage parallel and perpendicular to the direction of multiatomic steps

Previously, the mobility of N-polar HEMTs was observed to degrade with the increasing reverse bias on the gate.[20] From the energy band diagrams shown in the Fig. 2, it can be seen that the confinement for the electrons in the 2DEG increases with higher reverse bias on the gate and the electrons are pushed more against the AlGaN (or AlN) back barrier. Hence, a mobility degradation is expected with increasing reverse bias on the gate, because of increased alloy disorder scattering.[20] Introduction of an AlN interlayer can potentially mitigate such a degradation, by reducing the penetration of electron wave functions into the ternary AlGaN back barrier. Gated TLMs and C-V measurements have been performed on these devices to investigate the dependence of sheet resistance and electron mobility on reverse gate bias in both the directions (parallel and perpendicular to the multiatomic steps) and the influence of the AlN interlayer in mitigating this degradation. The resistance of TLM patterns with gate lengths varying from 2 to 20 μm, and access region lengths of 2 μm, was measured at different gate voltages (V_G). The slope of the resistance line with respect to the gate length multiplied by the gate width gave the channel sheet resistance R_{sh} at each gate bias. A small source current of 25 μA was used to avoid high-field effects and pinch-off of the channel. The 2DEG sheet charge n_s as a function of gate bias (V_G) was determined from C-V measurements. The mobility was calculated by combining the two measurements using

$$\mu_e(V_G) = \frac{1}{eR_{sh}(V_G)n_s(V_G)}. \quad (1)$$

Figure 6 shows the dependence of sheet resistance on carrier density as we deplete the channel, in a log scale. By com-

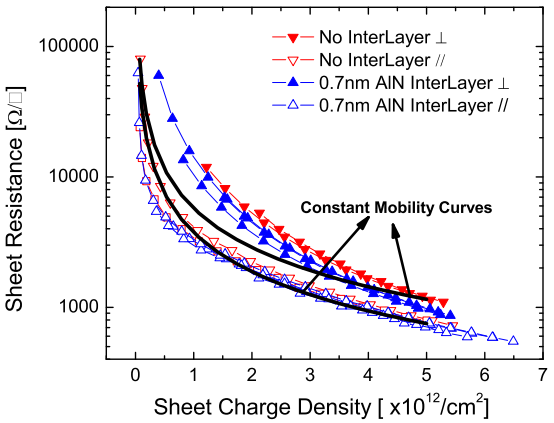

FIG. 6. (Color online) Dependence of sheet resistance on the carrier density (log scale). Constant mobility curves are shown as a reference.

paring with the constant mobility curves, it can be seen that the mobility degradation is higher in the direction perpendicular to steps, compared to the parallel direction. This can be attributed to an increased interface roughness scattering caused by multiatomic steps. Mobility as a function of charge was calculated from the gated TLM and C-V measurements and is plotted in Fig. 7, for one set of dies. It further confirms the lower degradation of mobility parallel to the steps as we deplete the charge and improvement of mobility with the introduction of an AlN Interlayer. The AlN interlayer, however, did not mitigate the mobility degradation with increasing reverse gate bias significantly. One possible reason for this observation could be that the thickness of the interlayer (0.7 nm) in our structure was not sufficient to prevent the increased random alloy scattering under high reverse gate bias. Further investigations, using samples with thicker AlN interlayers are under way.

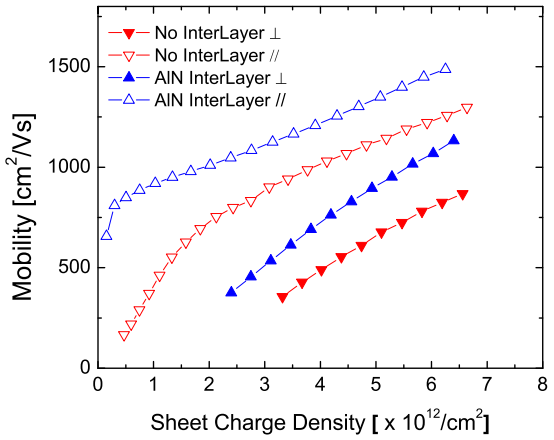

FIG. 7. (Color online) Dependence of mobility on the sheet charge density, obtained using gated TLM and C-V measurements

IV. CONCLUSION

In conclusion, it was demonstrated that the introduction of a 0.7 nm AlN interlayer improved the electron mobility in N-polar AlGaN/GaN HEMTs for conduction parallel and perpendicular to the multiatomic steps, similar to the observations in Ga-polar devices. The AlN interlayer, however, did not mitigate the mobility degradation with increasing reverse gate bias significantly. It was observed that orienting the devices such that the conduction is parallel to the multiatomic steps is beneficial for better electron transport and device performance. Qualitative explanations were provided for the trends observed in the device characteristics.

ACKNOWLEDGMENTS

The authors gratefully acknowledge the support of the ONR-MINE program supervised by Dr. Paul Maki and Dr. Harry Dietrich.

[1]U. Mishra, P. Parikh, and Y.-F. Wu, Proc. IEEE **90**, 1022 (2002).
[2]Y.-F. Wu, M. Moore, A. Saxler, T. Wisleder, and P. Parikh, "40–W/mm Double Field-plated GaN HEMTs," in *Device Research Conference, 2006 64th*, pp. 151–152, June 2006, State College, PA, USA (IEEE).
[3]Y. Pei, R. Chu, N. A. Fichtenbaum, Z. Chen, D. Brown, L. Shen, S. Keller, S. P. DenBaars, and U. K. Mishra, Jpn. J. Appl. Phys., Part 2 **46**, L1087 (2007).
[4]M. Higashiwaki, T. Mimura, and T. Matsui, Appl. Phys. Express **1**, 021103 (2008).
[5]M. H. Wong, Y. Pei, T. Palacios, L. Shen, A. Chakraborty, L. S. McCarthy, S. Keller, S. P. DenBaars, J. S. Speck, and U. K. Mishra, Appl. Phys. Lett. **91**, 232103 (2007).
[6]S. Rajan, Ph.D. thesis, University of California, 2006.
[7]S. Rajan, M. Wong, Y. Fu, F. Wu, J. S. Speck, and U. K. Mishra, Jpn. J. Appl. Phys., Part 2 **44**, L1478 (2005).
[8]R. Dimitrov, M. Murphy, J. Smart, W. Schaff, J. R. Shealy, L. F. Eastman, O. Ambacher, and M. Stutzmann, J. Appl. Phys. **87**, 3375 (2000).
[9]K. K. Rajan, M. J. Zhang, L.-C. Lim, Jpn. J. Appl. Phys., Part 1 **44**, 264 (2005).
[10]S. Keller, N. A. Fichtenbaum, F. Wu, D. Brown, A. Rosales, S. P. DenBaars, J. S. Speck, and U. K. Mishra, J. Appl. Phys. **102**, 083546 (2007).
[11]S. Keller, C. Suh, Z. Chen, R. Chu, S. Rajan, N. Fichtenbaum, M. Furukawa, S. DenBaars, J. Speck, and U. Mishra, J. Appl. Phys. **103**, 033708 (2008).
[12]M. H. Wong, Y. Pei, D. Brown, S. Keller, J. Speck, and U. Mishra, IEEE Electron Device Lett. **30**, 802 (2009).
[13]S. Kolluri, Y. Pei, S. Keller, S. Denbaars, and U. Mishra, IEEE Electron Device Lett. **30**, 584 (2009).
[14]I. P. Smorchkova, L. Chen, T. Mates, L. Shen, S. Heikman, B. Moran, S. Keller, S. P. DenBaars, J. S. Speck, and U. K. Mishra, J. Appl. Phys. **90**, 5196 (2001).
[15]S. Heikman, S. Keller, S. P. DenBaars, and U. K. Mishra, Appl. Phys. Lett. **81**, 439 (2002).
[16]M. Grundmann, BANDENG, http://my.ece.ucsb.edu/mgrundmann/bandeng.htm
[17]S. Rajan, Y. Hsieh, S. P. DenBaars, J. S. Speck, and U. K. Mishra, *2008 Electronic Materials Conference*, June 25–27, 2008, Santa Barbara, CA.
[18]D. Nath, S. Keller, Y. Hsieh, S. P. DenBaars, U. K. Mishra, and S. Rajan, "Lateral confinement of electrons in vicinal N-polar AlGaN/GaN heterostructure," e-print arXiv:1009.2537v1, Appl. Phys. Lett. (to be published).
[19]M. Akabori, J. Motohisa, and T. Fukui, J. Cryst. Growth **195**, 579 (1998).
[20]D. F. Brown, S. Rajan, S. Keller, Y.-H. Hsieh, S. P. DenBaars, and U. K. Mishra, Appl. Phys. Lett. **93**, 042104 (2008).